Analysis of Lloyd's mirror fringes for graded-index reflectors

John Lekner

Department of Physics, Victoria University of Wellington, Wellington, New Zealand

Received June 28, 1995; revised manuscript received February 5, 1996; accepted March 11, 1996

Measurement of the fringes produced by interference between direct and reflected light in the Lloyd mirror configuration can give information about the refractive-index profile of the reflecting surface, as has recently been shown. The experiment is performed near grazing incidence, and the analysis given so far has been based on the short-wave approximation, which is known to fail at grazing incidence, and no account has been taken of the difference between s and p polarizations. I give exact reflection phases for the solvable exponential refractive-index profile for both polarizations and develop general results for an arbitrary smooth profile that are valid near grazing incidence. I find that, for profiles that are slowly varying on the scale of the wavelength, the path-integral approximation to the phase is accurate except for the first few interference fringes, which come from glancing incidence reflections. The s and p phases are very nearly equal under the same conditions. Explicit formulas are given for dielectric function profiles that are linear or quadratic in the depth. The characteristic length of the quadratic profile may be found from the variation in the fringe spacing.

Key words: graded-index optics, integrated optics, waveguides, reflection, Lloyd's mirror.

1. INTRODUCTION

Klein, Opat, and collaborators have suggested[1] and implemented[2,3] a method of obtaining information about surfaces by measurement of the interference fringes produced in the Lloyd mirage configuration, so called because total reflection by a stratified medium near grazing incidence is precisely the mirage-producing situation. This method is one possible implementation of the holographic reconstruction idea put forward by Smith.[4] The analysis given[2,3] and the inversion method of Allen and Lipperheide[5] use the semiclassical short-wave approximation, in which the phase difference between the direct and the reflected waves is calculated along ray paths, as shown in Fig. 1.

The direct ray in Fig. 1 has length $L^2 + (H - h)^2$ and lies entirely in medium 1 of index n_1. The reflected ray has two straight parts that lie in medium 1, of lengths $\sqrt{L_1{}^2 + H^2}$ and $\sqrt{L_2{}^2 + h^2}$, plus a curved part along which the phase increment is, in the ray approximation,

$$\Delta_c \approx 2\frac{\omega}{c}\int_0^{z_0}\frac{n^2(z)dz}{\sqrt{n^2(z) - n^2(z_0)}} - \pi/2. \qquad (1)$$

A derivation of relation (1) is given below (see also Refs. 6 and 7); z_0 is the turning point at which the wave vector component perpendicular to the stratification (the z component) becomes zero. The transverse (x) component of the wave vector is constant by translational invariance in the x direction, which implies Snell's law,

$$n \cos \theta_1 = n(z)\cos \theta(z) = n(z_0), \qquad (2)$$

where θ_1 is the glancing angle of incidence and $\theta(z)$ is the glancing angle within the variable-index medium. Equation (2) defines z_0, which we see is a function of the angle of incidence. (We assume here that the refractive-index profile decreases monotonically with z, so that there is at most one turning point at each angle of incidence.) The normal component $q(z)$ of the wave vector is zero at the turning point:

$$q(z) = \frac{\omega}{c}n(z)\sin \theta(z) = \pm\frac{\omega}{c}\sqrt{n^2(z) - n^2(z_0)} \qquad (3)$$

[the second equality follows from Eq. (2)]. The phase increment along the curved part of the ray is $\int \mathbf{k}\cdot\mathbf{ds}$ where $\mathbf{k}$ is the wave vector and $\mathbf{ds}$ is an element of path length. This can be decomposed into contributions from motion in the x and z directions: let

$$K = \frac{\omega}{c}n_1 \cos \theta_1 = \frac{\omega}{c}n(z)\cos \theta(z) = \frac{\omega}{c}n(z_0) \qquad (4)$$

be the constant x component of the wave vector and (again in the ray approximation)

$$\Delta x \approx 2\int_0^{z_0}\frac{dz}{\tan \theta(z)} = 2n(z_0)\int_0^{z_0}\frac{dz}{\sqrt{n^2(z) - n^2(z_0)}} \qquad (5)$$

be the transverse displacement of the ray in the graded-index medium. Then

$$\Delta_c \approx K\Delta x + 2\int_0^{z_0}q(z)dz - \pi/2, \qquad (6)$$

which reduces to relation (1). The extra term $-\pi/2$ is a correction to the ray approximation, valid at short wavelengths for all dielectric function profiles that are smooth enough to be approximated by a linear variation in the neighborhood of the turning point [see, for example, Ref. 7, Sec. 6–7 and Eqs. (10.11)–(10.14)].

The phase difference between the reflected and the direct rays is

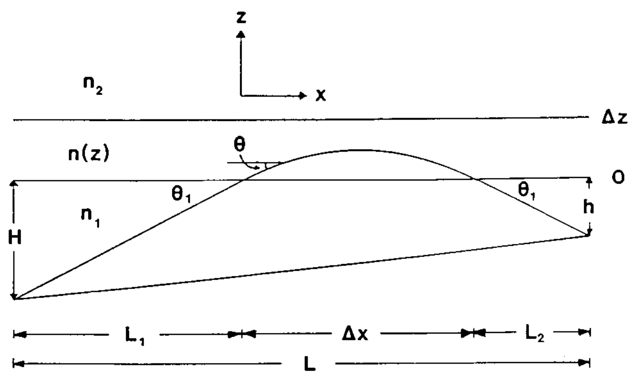

Fig. 1. Direct and reflected ray paths in a Lloyd's mirage configuration. The horizontal distance from source to detector is $L = L_1 + \Delta x + L_2$. The reflected ray path is drawn for indices $n_1 = 1.50$ and $n_2 = 1.49$, with a linear decrease in $n^2(z)$ from n_1^2 to n_2^2: $n_2(z) = n_1^2 + (n_2^2 - n_1^2)z/\Delta z$. For this profile the equation of the curved ray is $z = x(1 - x/\Delta x)\tan\theta_1$; the ray enters the variable index medium at $x = 0$ and $z = 0$ and exits at $x = \Delta x$ and $z = 0$, where $\Delta x = 4\Delta z \sin\theta_1 \cos\theta_1/\sin^2\theta_c$. The vertical scale is expanded: the actual glancing angle is $\theta_1 = 0.7\theta_c \approx 4.6°$, and $\Delta x \approx 24\Delta z$.

$$\begin{aligned}\Delta &= \Delta_c + \frac{\omega}{c}n_1\Big[\sqrt{L_1^2 + H^2} + \sqrt{L_2^2 + h^2} \\ &\quad - \sqrt{L^2 + (H - h)^2}\Big] \\ &= \Delta_c + \frac{\omega}{c}n_1\left[-\Delta x + \frac{2Hh}{L} + \frac{(H^2 + h^2)\Delta x}{2L^2}\right] \\ &\quad + O(L^{-3}).\end{aligned} \tag{7}$$

The variation of this phase difference with position on the screen (i.e., with h) leads to interference fringes. The quantity $2Hh/L$ is the leading term in the expansion of the geometric path difference, and by itself it would give a uniform fringe spacing. Variation of the fringe spacing thus may give information about the refractive-index profile, through Δ_c. The geometric and reflection phase contributions to the fringe spacing are considered in detail in Section 4.

2. COMPARISON OF EXACT RESULTS WITH THE SHORT-WAVE PHASE FORMULA

The interference pattern on the screen in Fig. 1 can in principle be found by solving the diffraction problem with a line source (a slit) and a gradient-index boundary. The ray approximation is the classical limit, and the short-wave result [relation (1)] for Δ_c approximates the ray locally by a plane wave with wave vector along the ray direction. In the formulas (1) and (6) no distinction is made between the s and p polarizations (i.e., between the TE and TM waves), and use is made of short-wave results near grazing incidence, where it is known that they fail (Ref. 7, p. 133). These approximations will be examined in this paper.

We will still assume that the cylindrical waves diverging from the line source can be approximated by plane waves. The term $\exp(iKx)$ represents the motion in the x direction throughout the stratification, giving a phase shift $K\Delta x$ for the curved part of the ray; we will therefore concentrate on the wave motion in the z direction. If the incoming plane wave is $\exp(iq_1z)$, the reflected wave will be (for s polarization) $r_s\exp(-iq_1z)$ in medium 1. In the total reflection situation ($n_1 > n_2$, $\cos\theta_1 > n_2/n_1$), $r_s = \exp(i\delta_s)$, where in the short-wave approximation[7]

$$\begin{aligned}\delta_s \approx \delta_a &= 2\int_0^{z_0} q(z)\mathrm{d}z - \pi/2 \\ &= 2\frac{\omega}{c}\int_0^{z_0}\mathrm{d}z\sqrt{n^2(z) - n^2(z_0)} - \pi/2.\end{aligned} \tag{8}$$

We assume that the refractive index decreases monotonically from n_1 at $z = 0$ to n_2 at $z = \Delta z$. Then at grazing incidence ($\theta_1 \to 0$) the turning point z_0 tends to zero, and the short-wave approximation to r_s tends to $-i$. This is wrong: It is known that at grazing incidence r_s always tends to -1 for all stratifications (Ref. 7, Sec. 2–3). Let $F(z)$ and $G(z)$ be two linearly independent solutions of the s-wave equation

$$\frac{\mathrm{d}^2E}{\mathrm{d}z^2} + q^2(z)E = 0 \tag{9}$$

in the range of variable index, namely, $0 \leqslant z \leqslant \Delta z$. Then, from Eq. (2.25) of Ref. 7,

$$r_s = \frac{q_1q_2(F, G) + iq_1(F, G') + iq_2(F', G) - (F', G')}{q_1q_2(F, G) + iq_1(F, G') - iq_2(F', G) + (F', G')}, \tag{10}$$

where

$$\begin{aligned}(F, G) &= F_1G_2 - G_1F_2, \quad (F, G') = F_1G_2' - G_1F_2', \\ (F', G) &= F_1'G_2 - G_1'F_2, \quad (F', G') = F_1'G_2' \\ &\quad - G_1'F_2',\end{aligned} \tag{11}$$

and $F_1 = F(0+)$, $F_2 = F(\Delta z-)$, F_1' is the derivative of $F(z)$ evaluated at $z = 0+$, etc.

It is immediately clear from Eq. (10) that $r_s \to -1$ as $q_1 \to 0$. When $n_1 > n_2$ and $\cos\theta_1 > n_2/n_1$, the normal component of the wave vector in medium 2 is imaginary:

$$q_2 = \frac{\omega}{c}\sqrt{n_2^2 - n_1^2\cos^2\theta_1} = i\frac{\omega}{c}\sqrt{n^2(z_0) - n_2^2} = i|q_2|. \tag{12}$$

In the total reflection situation the reflection amplitude thus takes the form

$$r_s = \frac{q_1[(F, G') + |q_2|(F, G)] + i[(F', G') + |q_2|(F', G)]}{q_1[(F, G') + |q_2|(F, G)] - i[(F', G') + |q_2|(F', G)]}. \tag{13}$$

The wave equation (9) is linear, with real coefficients, and thus the functions $F(z)$ and $G(z)$ may be taken to be real. Then Eq. (13) implies that

$$\delta_s = 2\arctan\left\{\frac{(F', G') + |q_2|(F', G')}{q_1[(F, G') + |q_2|(F, G)]}\right\}. \quad (14)$$

We see again that $r_s \to -1$ as $q_1 \to 0$, since $\delta_s \to \pm\pi$ at grazing incidence.

A comparison of the approximate δ_a [as given by relation (8)] with the exact phase [Eq. (14)] of the reflection amplitude has been given for the hyperbolic tangent profile in Fig. 6–9 of Ref. 7. Here we consider a refractive-index profile that is solvable for both s and p polarizations, namely, the exponential profile (see Sec. 2–5 of Ref. 7)

$$n(z) = \begin{cases} n_1 & z < 0 \\ n_1 \exp(z/b) & 0 \leqslant z \leqslant \Delta z, \\ n_2 & z > \Delta z \end{cases} \quad (15)$$

where $b = \Delta z/\log(n_2/n_1)$. The s-polarization solutions are Bessel functions $F(z) = J_s(u)$ and $G(z) = Y_s(u)$, with argument u and order s given by

$$u = n_1\frac{\omega}{c}|b|\exp(z/b), \quad s = K|b| = n(z_0)\frac{\omega}{c}|b|. \quad (16)$$

Note that the argument and the order are equal at the classical turning point $z = z_0$.

For p polarization the solutions are $uJ_p(u)$ and $uY_p(u)$, where

$$p^2 = (Kb)^2 + 1 = s^2 + 1. \quad (17)$$

From Eq. (2.98) of Ref. 7, we find that the p reflection phase is

$$\delta_p = 2\arctan\left\{\frac{(F', G') + (F, G')/u_1 + (F', G)/u_2 + (F, G)/u_1u_2 + |q_2|[(F', G) + (F, G)/u_1]}{q_1[(F, G') + (F, G)/u_2 + |q_2|(F, G)]}\right\}, \quad (18)$$

where now $F(z) = J_p(u)$ and $G(z) = Y_p(u)$. [From Eqs. (2.26) and (2.27) of Ref. 7 we see that the reflection amplitude for the normal component (E_z) of the electric field is $-r_p$ and that for the tangential component (E_x) it is r_p. At grazing incidence the normal component is dominant for the p wave, so the phases of r_s and $-r_p$ apply to the E_y and E_z components. Equation (18) gives the phase of $-r_p$.]

For the exponential profile, δ_a may be evaluated analytically. We find that

$$\delta_a = 2n_1\frac{\omega}{c}|b|(\sin\theta_1 - \theta_1\cos\theta_1) - \pi/2, \quad (19)$$

where θ_1 is the glancing angle of incidence and $n_1\cos\theta_1 = n(z_0)$. This formula applies in the total reflection region, where $\theta_1 < \arccos(n_2/n_1)$. Note that δ_a approaches $-\pi/2$ at grazing incidence, with $\delta_a + \pi/2$ tending to zero as $\frac{2}{3}n_1(\omega/c)|b|\theta_1^3$. The proportionality of the phase integral to the cube of the glancing angle of incidence near grazing incidence is universal for profiles that have a finite derivative at $z = 0$: From $n_1\cos\theta_1 = n(z_0)$ and $n(z) \approx n_1 - z|\mathrm{d}n/\mathrm{d}z|_{z=0}$ we find that

$$z_0 = \frac{n_1\theta_1^2}{2|\mathrm{d}n/\mathrm{d}z|_{z=0}} + O(\theta_1^4) \quad (20)$$

and thus that

$$\int_0^{z_0}\mathrm{d}z\,q(z) = \frac{\omega}{c}\int_0^{z_0}\mathrm{d}z\sqrt{n^2(z) - n^2(z_0)}$$

$$= \left(\frac{\frac{\omega}{c}n_1^2}{|\mathrm{d}n/\mathrm{d}z|_{z=0}}\right)\frac{\theta_1^3}{3} + O(\theta_1^5). \quad (21)$$

For such profiles, Eq. (20) shows that the Lloyd mirror experiment near grazing incidence probes only depths of order $\theta_1^2/|\mathrm{d}\log n/\mathrm{d}z|_{z=0}$.

More diffuse profiles can have zero first derivative at $z = 0$, and $n(z) \approx n_1 - 1/2z^2|\mathrm{d}^2n/\mathrm{d}z^2|_{z=0}$, in which case

$$z_0 = \left(\frac{n_1}{|\mathrm{d}^2n/\mathrm{d}z^2|_{z=0}}\right)^{1/2}\theta_1 + O(\theta_1^3), \quad (22)$$

and the phase integral is independent of the second derivative to leading order in θ_1:

$$\int_0^{z_0} q(z)\mathrm{d}z = \frac{\pi}{4}\frac{\omega}{c}n_1\theta_1 + O(\theta_1^3). \quad (23)$$

The short-wave approximation δ_a to the s wave reflection phase δ_s is compared with the exact phase in Fig. 2. We see that the short-wave approximation fails at grazing incidence but becomes accurate away from grazing incidence in cases (such as the example used here) in which the profile is smooth and thick on the scale of the wavelength. Note also that δ_s and δ_p agree closely in these circumstances (Appendix A gives the relationship between δ_s and δ_p for the exponential profile).

The exact s-wave phase is given by Eq. (14) and is seen to depend on solutions of the wave equation, and their derivatives, evaluated at the boundaries of the inhomogeneous reflecting region. The approximate s-wave phase $\delta_a = 2\int_0^{z_0}q(z)\mathrm{d}z - \pi/2$ integrates the phase increment $q(z)\mathrm{d}z$ only up to the turning point z_0. It takes no account of the evanescent penetration of the wave into the region beyond the classical turning point. It might be thought that the use of the full JWKB wave functions in Eq. (14) would lead to a phase δ_{sw}, which does not have the deficiencies of δ_a. We find, however, that although the resultant limiting value $r_s \to -1$ is in accord with the general theorem of Ref. 7 for reflection at grazing incidence, the improved short-wave phase δ_{sw} fails at small glancing angles, just as the simpler phase δ_a did. Neither δ_a nor δ_{sw} gives the correct linear variation of phase with glancing angle, which will be shown to be a general property in Section 3. Both fail because of the application of short-wave wave functions to a situation in which the problem has a long-wave character at glancing inci-

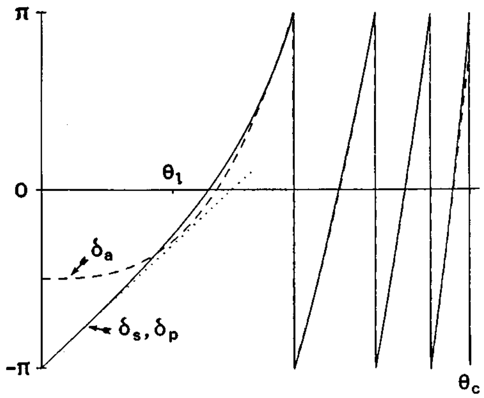

Fig. 2. Reflection amplitude phase for the exponential profile as a function of the glancing angle, from grazing incidence to the critical angle. The profile parameters are $n_1 = 1.50$, $n_2 = 1.49$, $\omega\Delta z/c = 100$. The layer thickness Δz is thus $50/\pi \approx 15.9$ vacuum wavelengths. The critical angle θ_c is $\sim 6.6°$, and according to Eq. (A13) the linear region extends to $\theta_l \approx 2°$. The dashed curve is the short-wave approximation δ_a of Eq. (19), and the dotted line is the glancing incidence variation [relations (33) and (34)]. The solid curve gives the exact δ_s and δ_p of Eqs. (14) and (18); for the profile parameters used, the s and p reflection phases are not distinguishable on this scale.

dence (where the normal component of the wave vector $q_1 \to 0$), even when $(\omega/c)\Delta z = 2\pi\Delta z/\lambda_{\text{vac}}$ is large.

3. REFLECTION PHASE NEAR GRAZING INCIDENCE

In this section it will be shown that the phase for small glancing angle θ_1 is linear in θ_1, and the coefficient of θ_1 will be evaluated for two classes of refractive-index profiles. Let us write Eq. (14) as

$$\delta_s = 2 \arctan(Q/q_1), \quad Q \equiv \frac{(F', G') + |q_2|(F', G)}{(F, G') + |q_2|(F, G)}. \tag{24}$$

From $\arctan(X) = \text{sgn}(X)\pi/2 - X^{-1} + O(X^{-3})$ we have

$$\delta_s = \text{sgn}(Q_0)\pi - 2q_1/Q_0 + O(q_1/Q_0)^3, \tag{25}$$

where Q_0 is the grazing incidence limiting value of Q. Since $q_1 = n_1(\omega/c)\sin\theta_1$, Eq. (25) shows that δ_s is linear in θ_1 small glancing angles, if Q_0 exists.

Next we consider profiles [such as the exponential profile of Eq. (15)] that are linear in z for small z. Near grazing incidence the normal component of the wave vector, $q(z) = n(z)(\omega/c)\sin\theta(z)$, is small, and the short-wave approximations fail. To solve wave equation (9) we assume that $n(z)$, and therefore also the dielectric function $\varepsilon(z) = n^2(z)$, are linear in z for small z. Near the turning point z_0 we have

$$q^2(z) \approx (z - z_0)\frac{\omega^2}{c^2}\left(\frac{d\varepsilon}{dz}\right)_{z_0}. \tag{26}$$

Define a dimensionless variable ζ by

$$\zeta = (z - z_0)k_0, \quad {k_0}^3 = \frac{\omega^2}{c^2}\left(-\frac{d\varepsilon}{dz}\right)_{z_0}. \tag{27}$$

Then wave equation (9) transforms to

$$\frac{d^2E}{d\zeta^2} - \zeta E = 0, \tag{28}$$

the solutions of which are the Airy functions $Ai(\zeta)$ and $Bi(\zeta)$. Thus $F(z) \approx Ai(\zeta)$, $G(z) \approx Bi(\zeta)$ are two linearly independent approximate solutions of the wave equation. These solutions are accurate near the turning point z_0, which is at small depths z near grazing incidence. The general formula (14) for δ_s requires evaluation of F and G and of their derivatives at $z = 0$ and $z = \Delta z$; the corresponding values of ζ are

$$\zeta_1 = -z_0k_0, \quad \zeta_2 = (\Delta z - z_0)k_0. \tag{29}$$

For all profiles, $z_0 \to 0$ at grazing incidence, so we are interested in the values of $Ai(\zeta)$ and $Bi(\zeta)$ and of their derivatives at $\zeta = 0$ and $\zeta = \Delta z k_0$. We assume that the profile characteristics and the wavelength of the light are such that $\Delta z k_0 \gg 1$; from the Airy function asymptotic forms[9]

$$Ai(\zeta) \sim 1/2\pi^{-1/2}\zeta^{-1/4}\exp(-2/3\zeta^{3/2}),$$
$$Bi(\zeta) \sim \pi^{-1/2}\zeta^{-1/4}\exp(2/3\zeta^{3/2}), \tag{30}$$

it follows that Bi dominates at the base of the inhomogeneous layer. The fact that the Airy functions do not provide an accurate solution for large z [except for the profiles for which $\epsilon(z)$ is linear in z at all z, for which the Airy functions are exact solutions[7]] does not matter: the solution that is accurately $Bi(\zeta)$ at small ζ will dominate at large ζ in all cases and cancel out from δ_s, as we shall see. At the turning point where $\zeta = 0$ we use the values[9]

$$c_1 = Ai(0) = Bi(0)/\sqrt{3} = [3^{2/3}\Gamma(2/3)]^{-1},$$
$$c_2 = -Ai'(0) = Bi'(0)\sqrt{3} = [3^{1/3}\Gamma(1/3)]^{-1}. \tag{31}$$

From Eqs. (30) and (31), neglecting terms of order $\exp[-4/3(\Delta z k_0)^{3/2}]$, we have

$$Q_0 \approx -\frac{c_2k_0}{c_1} = -\frac{3^{1/3}\Gamma(2/3)}{\Gamma(1/3)}k_0 \approx -0.729k_0. \tag{32}$$

We note that this negative value of Q_0 applies to all profiles for which $n(z)$ decreases linearly with z for small z. All such profiles therefore have linear variation of the reflection phase with the glancing angle:

$$\delta_s = -\pi + \left(\frac{2c_1}{c_2}\right)\left(\frac{\omega n_1}{ck_0}\right)\theta_1 + O({\theta_1}^3). \tag{33}$$

For exponential profile (15) the dimensionless parameter $\omega n_1/ck_0$ takes the grazing incidence value

$$\frac{\omega n_1}{ck_0} \to \left[\frac{n_1\omega\Delta z/c}{2\log(n_1/n_2)}\right]^{1/3}. \tag{34}$$

Figure 2 compared the s wave phase predicted by relations (33) and (34) with the exact phase for the exponential profile.

Another important class of profiles has $n(z)$ or $\varepsilon(z)$ quadratic in z at small z: Let

$$\varepsilon(z) = \varepsilon_1(1 - z^2/D^2) \tag{35}$$

and set

$$z = a\zeta, \qquad a^2 = \frac{D}{2n_1\omega/c}, \qquad \alpha = (aq_1)^2. \qquad (36)$$

Wave equation (9) then reduces to

$$\frac{d^2E}{d\zeta^2} + (\alpha - \zeta^2/4)E = 0, \qquad (37)$$

for which the standard solutions are parabolic cylinder functions[10] $U(-\alpha, \zeta)$, $V(-\alpha, \zeta)$. The function V dominates for large ζ:

$$U(-\alpha, \zeta) \sim \zeta^{\alpha-1/2}\exp(-1/4\zeta^2),$$
$$V(-\alpha, \zeta) \sim \left(\frac{2}{\pi}\right)^{1/2}\zeta^{-\alpha-1/2}\exp(1/4\zeta^2). \qquad (38)$$

Thus when $\Delta z/a \gg 1$ the grazing incidence limit of Q_0 is

$$Q_0 \approx \frac{1}{a}\frac{U'(0, 0)}{U(0, 0)} = -\frac{\sqrt{2}\Gamma(3/4)}{a\Gamma(1/4)} \approx -0.478/a \qquad (39)$$

[see Eqs. (19.3.5) of Ref. 10]. From Eq. (25) it follows that

$$\delta_s = -\pi + \frac{\Gamma(1/4)}{\Gamma(3/4)}(n_1\omega D/c)^{1/2}\theta_1 + O(\theta_1^{\,3}). \qquad (40)$$

For comparison, we rewrite the result [Eq. (33)] for linear variation in the dielectric function, $\varepsilon(z) = \varepsilon 1(1 - z/d + \ldots)$:

$$\delta_s = -\pi + \frac{2\Gamma(1/3)}{3^{1/3}\Gamma(2/3)}(n_1\omega d/c)^{1/3}\theta_1 + O(\theta_1^{\,3}). \qquad (41)$$

Provided that a limiting value of Q as $q_1 \to 0$ exists, the phase of the reflection amplitude is linear in the glancing angle θ_1. The coefficient of θ_1 is determined by the variation of $n(z)$ in the outer boundary of the reflecting layer. This may be expected on physical grounds, since the classical turning point z_0 approaches the outer boundary at grazing incidence, and the wave is evanescent beyond z_0.

4. LLOYD MIRAGE FRINGE SPACING

We have seen that the approximate short-wave phase δ_a given by relation (8) and the more complete δ_{sw} both fail at grazing incidence, though in different ways. Nevertheless, for profiles that are smooth and thick on the scale of the wavelength, the semiclassical phase δ_a is accurate in a large portion of the total reflection region, namely, for $\theta_l \lesssim \theta_1 \leqslant \theta_c$, where $\theta_l = (n_1\omega d/c)^{-1/3}$ or $\theta_l = (n_1\omega D/c)^{-1/2}$ for linear or quadratic variation of the index at small z, respectively. The interference fringe pattern is determined by the total phase given in Eq. (7), with $\Delta_c = K\Delta x + \delta_s$ for s-polarized light:

$$\Delta = \delta_s + K\Delta x + \frac{\omega}{c}n_1[\sqrt{L_1^{\,2} + H^2} + \sqrt{L_2^{\,2} + h^2} - \sqrt{L^2 + (H - h)^2}]. \qquad (42)$$

From Fig. 1 we see that

$$H/L_1 = \tan\theta_1 = h/L_2; \quad L_1 + \Delta x + L_2 = L, \qquad (43)$$

so that $h = (L - \Delta x)\tan\theta_1 - H$ and

$$L_1 = \frac{L - \Delta x}{1 + h/H}, \qquad L_2 = \left(\frac{h}{H}\right)\frac{L - \Delta x}{1 + h/H}. \qquad (44)$$

The expression in the square brackets in Eq. (42), which is the length of the straight-line parts of the reflected ray minus the length of the direct ray, is equal to

$$-\Delta x + \frac{2Hh}{L} + \frac{(H^2 + h^2)\Delta x}{2L^2} + O(L^{-3}). \qquad (45)$$

Thus, since $K = n_1(\omega/c)\cos\theta_1$,

$$\Delta = \delta_s + n_1\omega/c\left[(\cos\theta_1 - 1)\Delta x + \frac{2Hh}{L} + \frac{(H^2 + h^2)\Delta x}{2L^2}\right] + O(L^{-3}). \qquad (46)$$

The experimental results are photographs of fringes, seen as a function of h, which itself depends nonlinearly on the angle of incidence. Note that the lateral displacement Δx is a function of the angle of incidence: For linear variation of the dielectric function, $n^2(z) \equiv \varepsilon(z) = \varepsilon_1(1 - z/d)$, we find that $z_0 = d\sin^2\theta_1$, and the ray approximation gives

$$\Delta x \approx 2n(z_0)\int_{\theta_0}^{z_0}\frac{dz}{\sqrt{\varepsilon(z) - \varepsilon(z_0)}} = 4d\sin\theta_1\cos\theta_1,$$
$$\delta_s \approx \delta_a = -\frac{\pi}{2} + \frac{4}{3}(n_1\omega d/c)\sin^3\theta_1. \qquad (47)$$

For quadratic variation, $\varepsilon(z) = \varepsilon_1(1 - z^2/D^2)$, we have $z_0 = D\sin\theta_1$ and

$$\Delta x \approx \pi D\cos\theta_1,$$
$$\delta_s \approx \delta_a = -\frac{\pi}{2} + \frac{\pi}{2}(n_1\omega D/c)\sin^2\theta_1. \qquad (48)$$

When we put these expressions into Eq. (46) and write θ_1 in terms of h using $(L - \Delta x)\tan\theta_1 = H + h$,

$$\theta_1(\text{linear}) = \frac{H + h}{L} + O(L^{-3}),$$
$$\theta_1(\text{quadratic}) = \frac{H + h}{L}\left(1 - \frac{\pi D}{L}\right) + O(L^{-3}), \qquad (49)$$

we obtain the total phase shift as a function of the height above the surface, h. Each increase of Δ by 2π gives an additional fringe; the intensity is proportional to $|1 + \exp(i\Delta)|^2 = 4\cos^2(\Delta/2)$. We find that

$$\Delta(\text{linear}) \approx -\frac{\pi}{2} + 2n_1\frac{\omega}{c}\frac{Hh}{L} + O(L^{-3}), \qquad (50)$$

$$\Delta(\text{quadratic}) \approx -\frac{\pi}{2} + 2n_1\frac{\omega}{c}\frac{Hh}{L} + \frac{\pi}{2}n_1\frac{\omega}{c}D\frac{H^2 + h^2}{L^2} + O(L^{-3}). \qquad (51)$$

We see that, because of the extra factor of $\sin\theta_1$ in both δ_a and Δx for the linear profile, the fringe spacing

$$\Delta h \approx \frac{2\pi}{\mathrm{d}\Delta/\mathrm{d}h} \tag{52}$$

is constant at $\lambda_1 L/2H$ in the case of the linear profile ($\lambda_1 = \lambda/n_1$, where $\lambda = 2\pi c/\omega$ is the vacuum wavelength), whereas it is

$$\Delta h \approx \frac{\lambda_1 L}{2H + \pi Dh/L} \approx \frac{\lambda_1 L}{2H}\left(1 - \frac{\pi Dh}{2HL}\right) \tag{53}$$

for the quadratic profile. These results indicate that the two prototypical index profiles, respectively linear and quadratic in the depth, can be distinguished in the fringe pattern and that, further, the characteristic length D of the quadratic variation might be determined from the decrease in the fringe spacing with h.

5. SUMMARY AND CONCLUSION

We have seen that the path-integral formula for the reflection phase fails at grazing incidence but is otherwise accurate for profiles that are slowly varying on the scale of the wavelength. An improved short-wave approximation, which allows for penetration of the evanescent wave into the classically forbidden region, gives the correct phase at glancing incidence but does not give the correct angle dependence.

An exact solution (for both polarizations) of the wave equation for the exponential profile shows that the s and p phases are nearly the same under the same conditions that make the path-integral phase accurate.

All profiles give a reflection phase near glancing incidence that varies linearly with the glancing angle. Explicit formulas for this variation are given for linear and for quadratic variation of the dielectric function with depth.

The fringe spacing is found to be constant for linear profiles, equal to Young's two-slit fringe spacing $\lambda_1 L/2H$, when the total phase difference between the direct and reflected rays is calculated to order L^{-2}. For the quadratic profile there is a correction to the total phase of order L^{-2}, which could lead to the extraction of the profile characteristic length D, provided that the parameters of the experiment are chosen so as to make Dh/HL not too small compared to unity.

APPENDIX A: POLARIZATION DEPENDENCE OF THE REFLECTION PHASE

We will consider the s and p phases near grazing incidence. From Eqs. (1.26) and (1.27) of Ref. 7 we see that for p polarization the reflection amplitude is $-r_p$ for the normal component E_z of the electric field and that it is $+r_p$ for E_x. At grazing incidence the component E_z dominates; in this paper the reflection phases δ_s and δ_p are accordingly defined by

$$r_s = |r_s|\exp(i\delta_s), \qquad -r_p = |r_p|\exp(i\delta_p), \tag{A1}$$

for comparison of the phase of E_y (for the s wave) with the phase of the dominant p-wave component (E_z).

The simplest case to consider is that of a sharp transition between two media of indices n_1 and n_2. The reflection amplitudes are, in total reflection,

$$r_s = \frac{q_1 - i|q_2|}{q_1 + i|q_2|}, \qquad -r_p = \frac{q_1/\varepsilon_1 - i|q_2|/\varepsilon_2}{q_1/\varepsilon_1 + i|q_2|/\varepsilon_2}, \tag{A2}$$

where $\epsilon_1 = n_1{}^2$ and $\epsilon_2 = n_2{}^2$ are the dielectric constants of the two media, $q_1 = n_1(\omega/c)\sin\theta_1$ and $|q_2| = (\omega/c)\sqrt{\varepsilon_1\cos^2\theta_1 - \varepsilon_2}$ for $\theta_1 < \theta_c = \arccos(n_2/n_1)$.

Thus

$$\delta_p - \delta_s = 2\left[\arctan\left(\frac{|q_2|}{q_1}\right) - \arctan\left(\frac{\varepsilon_1|q_2|}{\varepsilon_2 q_1}\right)\right]. \tag{A3}$$

This phase difference is zero at glancing incidence where $q_1 \to 0$. The phase difference has maximum magnitude at glancing angle θ_m given by

$$\sin^2\theta_m = \frac{\varepsilon_1 - \varepsilon_2}{\varepsilon_1 + \varepsilon_2}. \tag{A4}$$

At θ_m, the phase difference is

$$(\delta_p - \delta_s)_{\theta_m} = 4\ \arctan\left(\frac{n_2}{n_1}\right) - \pi. \tag{A5}$$

[Compare Eqs. (10.30)–(10.32) of Ref. 7.] From $\arctan(X) = \mathrm{sgn}(X)\pi/2 - X^{-1} + O(X^{-3})$ and Eq. (A3) we see that the phase difference is linear in glancing angle θ_1 for a small glancing angle:

$$\delta_p - \delta_s = -\left(\frac{\varepsilon_1 - \varepsilon_2}{\varepsilon_1}\right)^{1/2}\theta_1 + O(\theta_1{}^3). \tag{A6}$$

We conclude from Eqs. (A5) and (A6) that, for a sharp transition, the phase difference near grazing incidence between the reflected p and s polarizations will be negligible only if $n_2 \approx n_1$.

Next we look at the opposite case of a slow transition between the media of indices n_1 and n_2, taking the exponential profile defined in Eq. (15) as a specific example. For s polarization the solutions are $F(z) = J_s(u)$ and $G(z) = Y_s(u)$; these functions and their derivatives are to be evaluated at the end points

$$u_1 = n_1|b|\omega/c, \qquad u_2 = n_2|b|\omega/c, \tag{A7}$$

where $b = \Delta z/\log(n_2/n_1)$. The order s of the Bessel functions is $s = K|b| = n_1|b|(\omega/c)\cos\theta_1$, and at grazing incidence this tends to u_1. If $\omega\Delta z/c \gg 1$ or if $n_2 \approx n_1$ (i.e., if the index variation is slow on the scale of the wavelength or if it is small), u_1 and u_2 will be large. Also $n_1 > n_2$, so $u_1 > u_2$; thus at grazing incidence, $F_2 = J_{u_1}(u_2)$ will be small and $G_2 = Y_{u_1}(u_2)$ will be large. From Eqs. (9.3.7) and (9.3.8) of Ref. 11 we find that

$$F_2/G_2 \sim -\frac{1}{2}\exp[-2u_1(\alpha - \tanh\alpha)] \equiv \sigma, \tag{A8}$$

where $\mathrm{sech}\,\alpha = n_2/n_1$. Thus G_2 dominates exponentially over F_2, and the same is true for the derivatives $G_2{}'$ and $F_2{}'$. The general formula (14) then simplifies to

$$\delta_s = \arctan(F_1{}'/q_1 F_1) + O(\sigma). \tag{A9}$$

Similarly, the p polarization phase shift, given by Eq. (18), simplifies to

$$\delta_p = \arctan(F_1{}' q_1 F_1) + O(\sigma) + O(u_1{}^{-1}) + O(u_2{}^{-1}) \tag{A10}$$

Thus the s and p reflection phases differ (near grazing incidence) only by the exponentially small factor σ and by terms of order $u_1{}^{-1}$ and $u_2{}^{-1}$. Near equality of δ_s and δ_p at glancing incidence can similarly be expected for any smooth and slowly varying profile.

Note that the result (A9) together with Bessel asymptotics enables us to check the general formula for the s-polarization phase shift at glancing incidence: From Eqs. (9.3.23) and (9.3.27) of Ref. 11 we find (see also Watson,[12] p. 232) that

$$\frac{J_v{}'(v)}{J_v(v)} = \left(\frac{6}{v}\right)^{1/3} \frac{\Gamma(2/3)}{\Gamma(1/3)} + O(v^{-1}). \tag{A11}$$

This result used in Eq. (A9), together with Eqs. (31), gives us

$$\delta_s = -\pi + \frac{2\Gamma(1/3)}{6^{1/3}\Gamma(2/3)}(n_1|b|\omega/c)^{1/3}\theta_1 + O(\sigma) + O(u_1{}^{-1}) + O(\theta_1{}^3), \tag{A12}$$

in agreement with Eq. (41), since $d = |b|/2$. The angular extent of the region where δ_s is linear in θ_1 is thus from zero (glancing incidence) to approximately

$$\theta_l = (n_1|b|\omega/c)^{-1/3} = \left[\frac{\log(n_1/n_2)}{n_1\Delta z\,\omega/c}\right]^{1/3}. \tag{A13}$$

REFERENCES

1. V. P. Gudkov, G. I. Opat, and A. G. Klein, "Neuron reflection interferometry: physical principles of surface analysis with phase information," J. Phys. Condens. Matter **5**, 9013–9024 (1993).
2. B. E. Allman, A. G. Klein, K. A. Nugent, and G. I. Opat, "Lloyd's mirage: a variant of Lloyd's mirror," Eur. J. Phys. **14**, 272–276 (1993).
3. B. E. Allman, A. G. Klein, K. A. Nugent, and G. I. Opat, "Refractive-index profile determinations by using Lloyd's mirage," Appl. Opt. **33**, 1806–1811 (1994).
4. P. R. Smith, "Reconstructing optical parameters from holographic amplitude data," Inverse Probl. **8**, 309–320 (1992).
5. L. J. Allen and R. Lipperheide, "Graded-index profiles by inversion with Lloyd's mirage," Appl. Opt. **35**, 3496–3499 (1996).
6. A. W. Snyder and J. D. Love, *Optical Waveguide Theory* (Chapman and Hall, London, 1983), pp. 13–20.
7. J. Lekner, *Theory of Reflection* (Nijhoff/Kluwer, Dordrecht, The Netherlands, 1987).
8. See, for example, E. Merzbacher, *Quantum Mechanics*, 2nd ed. (Wiley, New York, 1970), Secs. 7.2 and 7.5.
9. H. A. Antosiewicz, Chap. 10 in *Handbook of Mathematical Functions*, M. Abramowitz and I. A. Stegun, eds. (U.S. Government Printing Office, Washington, D.C., 1964).
10. J. C. P. Miller, Chap. 19 of Ref. 9.
11. F. W. J. Olver, Chap. 9 of Ref. 9.
12. G. C. Watson, *Theory of Bessel Functions*, 2nd ed. (Cambridge U. Press, Cambridge, 1966).